



Published in final edited form as:

Otol Neurotol. 2017 March ; 38(3): 339–346. doi:10.1097/MAO.0000000000001329.

Automatic cochlear duct length estimation for selection of cochlear implant electrode arrays

Alejandro Rivas, MD², Ahmet Cakir, MRes¹, Jacob B. Hunter, MD², Robert F. Labadie, MD PhD², M. Geraldine Zuniga, MD², George B. Wanna, MD², Benoit M. Dawant, PhD¹, and Jack H. Noble, PhD¹

¹Department of Electrical Engineering and Computer Science, Vanderbilt University, Nashville, TN 37232

²Department of Otolaryngology-Head and Neck Surgery Vanderbilt University Medical Center, Nashville, TN 37232

Keywords

Cochlear implant; electrode array selection; cochlea size; cochlear duct length

INTRODUCTION

The human cochlea and cochlear duct (CD), defined as the length of the scala media, are fully formed at birth. In 1938, Hardy first reported the histologic measurements of the cochlear duct length (CDL) in 68 cadaveric specimens via graphic reconstructions of serial sections, measuring from the middle of the round window to the helicotrema¹. Since the advent of cochlear implantation, multiple studies have assessed the role of using the CDL to determine the appropriate electrode length for implantation. This is particularly important as the length of the cochlea can vary between 25 – 45 mm in patients^{2–12}.

Several studies have demonstrated that greater angular insertion depths result in improved speech perception performance^{13–16}. Since the angular depth of insertion is dependent upon CDL and the length of the implanted electrode, the variability in CDL and electrode options can influence speech perception performance. In addition, as evidence suggests atraumatic cochlear implantation preserves residual hearing and postoperative performance, knowing the correct CDL is of paramount importance to ensure trauma caused by over-insertion (e.g. scalar translocation) is avoided.

Recently, building on the work of Hardy¹ and others⁸, Alexiades et al. described a simplified formula to calculate CDL at a given angular depth using computerized tomography (CT) and by measuring the distance from the middle of the round window (RW) to the farthest point

CORRESPONDING AUTHOR: Ahmet Cakir, MRes., Department of Electrical Engineering and Computer Science, 2301 Vanderbilt Pl., Box 1679 Station B, Nashville, TN 37235-1679, Telephone: 615-322-8478, Fax: 625-343-5459, ahmet.cakir@vanderbilt.edu, co-first-authorship

IRB APPROVAL: This study was approved by the Vanderbilt IRB 090155.

on the opposite wall of the cochlea, denoted A ¹⁷. However, this method remains time consuming and operator dependent, and intra- or inter-observer variability in measurements have not been studied.

Thus, herein we have developed an automatic method to measure both A and CDL at a given angular depth using an active shape model-based, automatic cochlea segmentation technique¹⁸. In the current work, we assess the inter-observer variability by computing differences between measurements of A across expert observers. We also compare expert measurements to automatic measurements of A , and investigate the sensitivity of the choice of electrode type to the choice of CDL measurement method by counting how often the choice of electrode would differ when different expert or automatic measurements are used to estimate CDL.

METHODS

After Institutional Review Board approval, we retrospectively reviewed a CT imaging database to identify 275 pre-operative CT scans that were available for review for adult patients who underwent cochlear implantation. As described in the following sub-sections, CDL was measured in each of these CTs using manual and automatic measurement methods.

Cochlear Duct Length from A

Previous literature has shown that A , the length of the line from the center of the round window (RW) through the modiolus to the farthest point on the lateral wall of the basal turn of the cochlea, can be used to calculate the length of the cochlear duct along the outer wall of the cochlea from the center of the RW to a specified angular depth¹⁹. The formula is defined as follows:

$$CDL(A, \theta) = 2.62A \log_e \left(1.0 + \frac{\theta}{235^\circ} \right), \quad (1)$$

where θ is the angular depth within the cochlea at which we want to estimate the CDL. The angular depth of a point in the cochlea is defined as proposed by Verbist et al²⁰. It is measured using the position of the mid-modiolar axis and the center of the round window membrane, as shown in Figure 1, which are found automatically using the automatic image processing methods described below. The middle of the round window membrane defines the 0° depth, and the angular depth of a point is measured as its angle around the mid-modiolar axis along the length of the cochlea spiral relative to the round window reference angle. 0° to 360° corresponds to the first turn of the cochlea, 360° to 720° corresponds to the second turn, etc. The angular depth where the cochlear duct ends is approximately 2.5 turns but this varies across subjects. Since advancement of the arrays past 2 turns (2T) is rare, and estimation of CDL at 2T is more reliable than that of the full CDL¹⁷, in this work we choose to estimate CDL at 2T rather than the full CDL. Measuring CDL along the outer wall of the cochlea to a depth of 2T implies $\theta = 720^\circ$, and thus Eqn. (1) simplifies to

$2.62A \log_e(1.0 + \frac{720}{235}) = 3.67A$. Further, Alexiades et al. showed that Eqn. (1) could be modified to calculate the length an electrode array with average diameter d would need to have to reach a specified depth as¹⁷:

$$E(A, \theta, d) = 2.62(A - d) \log_e(1.0 + \frac{\theta}{235c}) \quad (2)$$

Manual Measurement of A

Manual measurement of patient-specific A values was done using a software package developed in-house that allows for rotation of the CT volume to create oblique axial, coronal, and sagittal reconstructions as well as 3D views and permits selecting the RW and lateral wall points. Two fellowship-trained neurotologists independently reviewed each patient's imaging study, identifying the RW and the farthest point on the opposite wall of the cochlea for which a straight line could be drawn through the modiolus. The manually measured A values were denoted as A_{S1} for surgeon 1 and A_{S2} for surgeon 2. An example result of this process is shown in Figure 2. Using equation (1) with $\theta = 720^\circ$, the CDL along the outer wall at 2T can be computed for both A_{S1} and A_{S2} , and these quantities are denoted as CDL_{S1} and CDL_{S2} , respectively.

Automatic Measurement of A

Automatic segmentation of the cochlea was achieved by implementing the model fitting-based approach described by Noble et al., which was shown to localize highly accurate surface models of cochlear anatomy in patient CTs^{18,21}. This method permits accurately identifying anatomical sites anywhere on the surface of the cochlea. Thus, we used this approach to automatically identify a point on the middle of the RW and another point on the lateral wall of the first turn of the cochlea that is farthest from the RW. We then computed the distance between these two points for each patient. The automatically measured A values were denoted as A_{Auto} . All automatic cochlea segmentations were visually inspected in the patient CT image and confirmed to be accurate. Using equation (1), the corresponding CDL at 2T can be computed for A_{Auto} as CDL_{A-Auto} .

Automatic Direct Measurement of CDL at 2T

In addition to computing the CDL at 2T automatically as CDL_{A-Auto} by using equation (1) with A_{Auto} we can also use the automatic segmentation method to directly measure the CDL at 2T. Points along the outer wall of the cochlea along the CD were identified in the cochlea model to form the model CD curve. These points were automatically mapped to each patient CT using the model²². Then for each patient, we directly measure the outer wall CDL at 2T, $CDL_{Direct-Auto}$ by computing the length of the CDL curve defined by the model from RW to an angular depth of 2T.

Effect of CDL Measurement Approach on Selection of Array Type

While many factors go into the decision about what electrode array is most suitable for a patient, we investigated whether the choice of CDL measurement could affect selection of

the electrode array when only CDL is considered. To do this, we assessed how often CDL measurement would result in a different choice of electrode array between two array types, the Med-El (Innsbruck, Austria) *Flex24*TM (Array 1) and *Flex28*TM (Array 2). Array 1 and Array 2 both have 12 electrodes and average diameter of approximately 0.6 mm, and lengths of 24 and 28 mm, respectively. With lateral wall arrays, studies have shown a trend of deeper implantation being associated with better outcomes, suggesting that in general longer arrays are better, although several additional factors should be considered when selecting the electrode array. A smaller CDL warrants a shorter electrode to ensure the base of the array can be fully inserted and all basal electrodes are available for stimulation. Basal contacts that are too shallow and lie either near the entrance of the cochlea or outside the cochlea typically provide ineffective stimulation due to lack of access to neural populations. Such contacts are sometimes deactivated during cochlear implant (CI) programming but often are left at default values due to adequate volume perception potentially leading to sub-optimal hearing outcomes by interfering with other electrodes. On the other hand, a larger CDL warrants a longer electrode to ensure the tip of the array can reach apical stimulation sites which has also been shown to be important in maximizing audiological outcomes¹⁶. Given that there has been little evidence on what electrode depth is best for optimal hearing outcomes, the specific threshold value of A ($thresh-A$) used to decide between Array 1 and Array 2 is a matter of surgeon preference. Thus, in this work, we aim to show how often the choice of array would differ over a range of choices of $thresh-A$ across different techniques for measuring cochlea size when only cochlea size is used to make this decision. We tested the range of values of $thresh-A$ from 8 mm (CDL at $2T = 29.54$ mm) to 10.25 mm (CDL at $2T = 37.66$ mm) as this matches the range of A values in our dataset. The different measures of cochlea size described in the previous sub-sections, CDL_{S1} , CDL_{S2} , CDL_{A-Auto} , and $CDL_{Direct-Auto}$ were each used to estimate A for each case. Then, for each value of $thresh-A$, we counted how many times the different measures of cochlea size would lead to a different choice in the array that is selected.

Statistical Analysis

Continuous features were described with means, ranges, and standard deviations. Analysis of variance (ANOVA) with post-hoc comparison analysis was performed to compare means. Inter-observer variability in measurement of cochlea size were assessed with mean differences, mean absolute differences, and maximum absolute differences. Fisher's exact tests were used to determine if measurement techniques influenced appropriate electrode selection. p -values less than 0.05 were considered statistically significant.

RESULTS

The mean, range, and standard deviations for length A for A_{Auto} , A_{S1} and A_{S2} are shown in Table 1. A one-way repeated measures ANOVA revealed significant differences between the three different measurement means for the 309 ears ($p < 0.001$). Post-hoc analyses were conducted in order to assess the significant difference between each of the measurements. The three paired t-tests revealed that the means were significantly different ($p < 0.001$) between each pair of measurements. The mean difference, mean absolute difference, and the maximum absolute difference between the manual measurements A_{S1} and A_{S2} were, 0.06

mm, 0.18 mm, and 2.18 mm, respectively. The same measurements between A_{Auto} and A_{S1} were 0.18 mm, 0.25 mm, and 1.92 mm, and between A_{Auto} and A_{S2} were 0.12 mm, 0.18 mm, and 1.92 mm, respectively.

The mean and standard deviations for CDL_{S1} , CDL_{S2} , CDL_{A-Auto} , and $CDL_{Direct-Auto}$ were 32.71 ± 1.80 , 33.07 ± 1.69 , 33.87 ± 1.61 , and 34.14 ± 1.75 mm, respectively. A box plot of these measurements is displayed in Figure 3 where each of the box-plot represents a different measurement. In each boxplot, the box represents the inter-quartile range, the black line is the median, values that fall 1.5 times the interquartile range above the third quartile or below the first quartile are considered outliers and shown as circles, and the “whiskers” at the bottom and at the top represent the minimum and the maximum values excluding the outliers, respectively. Comparing the means, an ANOVA test revealed a significant difference between the four measurement means ($p < 0.001$). Post-hoc analyses were conducted. The paired t-tests between the six combinations of measures showed that each pair of measurements were significantly different ($p < 0.001$). Figure 3 illustrates that manually measuring A tends to underestimate A in comparison to automated techniques, resulting in an underestimation of the CDL. A comparison between different CDL measurements is shown in Figure 4 where each boxplot represents the absolute values of the differences between various CDL measurements. For instance, the first boxplot on the left corresponds to the absolute difference between $CDL_{Direct-Auto}$ and CDL_{A-Auto} . The boxplot is defined in the same way as previously explained. As illustrated by the boxplot, the $CDL_{Direct-Auto}$ and the CDL_{A-Auto} measurements are highly similar, with a mean difference, mean absolute difference, and maximum absolute difference of 0.27 mm, 0.35 mm, and 1.35 mm, respectively. The same measurements between automatic and manual measurements, on the other hand, have relatively high values, with mean absolute differences greater than 1.4 mm. In addition, the maximum and mean absolute differences between the manual CDL estimations have relatively high values of 8 and 1.15 mm, respectively, showing high inter-observer variability in the manual measurements.

In the left column of Figure 5, each panel corresponds to one measurement technique and shows the number of ears for which a different electrode array would be selected when using each other measurement method to measure A across the range of values of $thresh-A$. In the right column of Figure 5, a histogram of cochlea size across subjects is shown as measured using each of the measurement techniques. Equation (1) was used to map values between CDL at 2T and A . It is clear from the two upper plots in the left column that using $CDL_{Direct-Auto}$ or CDL_{A-Auto} measurements resulted approximately in the same electrode array type selections, with the biggest difference of 38 ears out of 309 occurring at a $thresh-A$ of 9.74 mm. Automated techniques to measure length A and CDL did not lead to significant differences in the selected electrode array type for any value of $thresh-A$ smaller than 9.5 mm ($p > 0.68$). Manual measurements by the first and second surgeon, on the other hand, led to a larger number of differences in the selected electrode array type between each other and the automated measures, as observed in Figure 5. The selections by the first surgeon were significantly different than the selections by the $CDL_{Direct-Auto}$ for all values of $thresh-A$ smaller than 10 mm ($p < 0.015$). When comparing selections based on measurements done by the second surgeon with those by $CDL_{Direct-Auto}$, Fisher’s exact test

revealed statistically significant differences between these two selections for *thresh-A* greater than 8.34 and smaller than 9.84 mm ($p < 0.02$).

DISCUSSION

Several studies have documented a correlation between the angular depth of insertion and speech performance outcomes following cochlear implantation^{13–16}. The angular depth of insertion is dependent on CDL and length of the electrode array^{12–17}. Choosing the appropriate length CI electrode array could ensure the desired angular depth of insertion, which in turn can improve postoperative hearing outcomes. The importance of the relationship between CDL and electrode length deals with cochlear coverage. An ideal electrode covers the entire frequency spectrum of the cochlea. Electrodes that are too short fail to reach the apical cochlea, possibly leading to poorer patient outcomes. On the other hand, electrodes that are too long may lead to cochlear trauma, leading to poorer patient outcomes; or under-insertion at the basal end, leading to a loss of coverage of the high-frequency spectrum also leading to poorer outcomes. Thus, an ideal fit between the electrode and the CDL is desired. Given these findings, determining the CDL and selecting the most appropriately sized electrode is important in maximizing patient benefit. Nonetheless, while several studies have described techniques in determining CDL, these techniques remain burdensome and time consuming with unknown intra- and inter-observer variability. Thus, we developed an automatic method measuring both length *A* and 2T CDL using an automatic model-based segmentation technique and compared it to previous reported techniques.

The results presented herein will permit weighing the importance of choice of measurement method when using cochlear size to choose between different array lengths for a specific subject and choice of *thresh-A*. Our long-term goal is to develop a system to assist with patient-customized selection of electrode arrays using comprehensive information including but not limited to the patient's CDL. In ongoing investigation, preliminary results indicate that a reasonable choice for *thresh-A* would be 8.5 mm. To arrive at this value, we have reviewed post-implantation CTs of 10 subjects in our CT imaging database who were implanted by multiple surgeons and with Array 2. We found that the base of the array was not fully inserted in 7 cases, leaving the most basal contact(s) ineffective. Further advancement of the array was not done due to the perception of resistance to avoid the risk of trauma. We speculate that deeper angular depths increase the likelihood resistance is encountered due to the increased redirection of forces necessary to advance the array as the coiling of the array increases (i.e. additive frictional forces as more of the electrode array abuts against intracochlear anatomy).

The average depth of the apical electrode across these 10 cases was 560°, thus we assume this is the angular depth at which resistance is encountered for the average cochlea. To establish a minimum target insertion depth, we further examined insertion depth in relation to consonant-nucleus-consonant (CNC) word scores²⁴ for 16 subjects including the 10 subjects implanted with Array 2 mentioned above as well as other subjects implanted with long electrodes from the same manufacturer. These data are shown in Supplemental Figure 1. As seen in the red curve in the figure, the trend is that increasing angular depth is

associated with better CNC scores, however that trend appears to plateau once the insertion depth passes 450 degrees, suggesting that this insertion depth is deep enough to expect maximal outcomes. Thus, our strategy would be to choose *thresh-A* such that the array we select is long enough to at least reach a 450 degree depth at full insertion and is short enough to permit having all basal electrodes inserted into the cochlea when the tip insertion depth reaches 560 degrees. At *thresh-A* = 8.5 mm, eqn. (2) predicts the length of the intra-cochlear path of Array 2 to reach depth to be 25 mm for cochleae of that size. For the reader's reference, angular insertion depths predicted by eqn. (2) for Array 1 and Array 2 for cochleae of different sizes are shown in Supplemental Figure 2 for "full-insertion," where the depth marker on the array reaches the RW, as well as for an insertion where the 12th electrode is located at RW, denoted as "under-insertion." The lengths of the electrode arrays between the tip and the 12th electrode are approximately 21 mm and 24 mm, for Array 1 and Array 2, respectively. Thus, insertion depth for a full-insertion Array 1 and for an under-insertion Array 2 is the same, as shown in the figure. Since Array 2 is 28 mm in length with contacts distributed on the apical 24 mm of that length, it is likely that the array will be under-inserted at the base for cochleae that are smaller than $A=8.5\text{mm}$. For smaller cochlea, it is reasonable to consider Array 1 instead. At full-insertion, Array 1 would be predicted to reach 515°, which is deep enough that we would not expect a detriment to outcomes due to lack of insertion depth. For cochleae with A greater than 8.5 mm, Array 2 would be the preferred choice to ensure greater insertion depths can be reached. From Figure 5, it can be seen that Array 2 would be selected in 291/309 cases when using CDL_{A-Auto} , and it can be seen that the choice of array would differ in 53 and 30 of the 309 cases when using CDL_{S1} and CDL_{S2} , respectively. For cochleostomy (C) insertion on the other hand, *thresh-A* = 9 mm (CDL at 2T = 33.1 mm) could be used as the intra-cochlear path of the array will be around 1.5 mm shorter for cochleostomy insertions, and thus the *thresh-A* value needs to be appropriately adjusted. With *thresh-A* = 9 mm, Figure 5 shows that Array 2 would be selected in 211/309 cases when using CDL_{A-Auto} , and it can be seen that the choice of array would differ in 115 and 80 of the 309 cases when using CDL_{S1} and CDL_{S2} , respectively. Future temporal bone studies would be necessary to assess the effectiveness of these choices for *thresh-A*.

While Escude et al. described the length of the cochlear lateral wall based on the length A^{19} , we noted significant inter-observer variability between manual measurements conducted by fellowship trained neurotologists. When we automated the measurement, we noted further significant differences between all three measurements. Rather than continuing to measure an indirect metric of CDL, we automatically segmented CDL and measured its length directly. There were significant differences between the automatic CDL measure and the calculated CDLs utilizing the manual A measurements. Ignoring all other factors that influence electrode selection, we found that the significant difference in CDL measurement techniques might lead to different clinical decisions across the range of possible choices for *thresh-A*.

Figure 3 and the histograms in Figure 5 illustrate that the surgeons tend to underestimate the A value, in turn causing underestimation of CDL. Statistically significant differences between surgeons for both approaches can be explained by multiple factors. First, the measurement requires identification of the RW, modiolus, and the opposite lateral wall of the

cochlea. However, the slice containing all three anatomic landmarks is not available within normal coronal, axial or sagittal views, thus requiring specific reformatting; and difficulties in reformatting can lead to possible measurement errors. Second, once familiar with the reformatting approach, we estimate that it took approximately 90 seconds per ear to identify the appropriate angle and measure A . We estimate an even longer process would be necessary in clinical practice where less optimized CT analysis programs are available and familiarity with the software is rare.

Because of the large variability in the measurement of A value and its possible implication on the choice of the electrode clinically selected, a more consistent, less time consuming and reproducible method to determine CDL would be of high utility. The current study shows that an automatically selected A could achieve these desired qualities requiring ~30 seconds processing time on a standard PC. In determining CDL, there was no significant difference when using $CDL_{Direct-Auto}$ or CDL_{A-Auto} calculations regarding chosen electrode type when $thresh-A$ of less than 9.5 mm is used. While future studies will be required to better understand the differences between the CDL_{A-Auto} and $CDL_{Direct-Auto}$ measurements, the results presented highlight the role an automated system may have in selecting electrode array types.

There were several limitations to our study. First, ideally these measurement techniques should be correlated with histopathologic and/or microCT datasets. Second, we recognize that multiple factors are considered in determining the appropriate electrode for each patient including residual hearing, etiology of hearing loss, and duration of hearing loss to name but a few. Volume and cross-sectional area of the scala tympani are other factors that might be important for electrode selection, although recent studies have not found volume to be significantly associated with scalar translocations²³. In this study, those variables were ignored as our aim was to evaluate variability due to choice of CDL measurement technique alone. However, it is likely that volume and cross-sectional area are correlated with CDL, and this relationship will be investigated in future work.

CONCLUSIONS

Choosing the best CI electrode array for a patient is an important task for optimizing hearing outcomes. A -values measured manually are user-dependent, and errors in measurement of A impact upon the choice of length of CI electrode array for certain patients. Measuring A and CDL automatically is less time consuming and generates more repeatable results. Our automatic approach could make the use of CDL for patient-customized treatment more clinically adoptable.

Supplementary Material

Refer to Web version on PubMed Central for supplementary material.

Acknowledgments

CONFLICTS OF INTEREST/DISCLOSURES: Dr. Wanna is a consultant for MED-EL, Advanced Bionics, Oticon Medical, and Cochlear Americas. Dr. Rivas is a consultant for MED-EL, Advanced Bionics, Cochlear Americas, Stryker, Olympus and Grace Medical. Dr. Labadie is a consultant for Advanced Bionics and Ototronix.

FUNDING: The project was supported by grants R01DC014037, R01DC008408, R01DC014462 from the National Institute on Deafness and Other Communication Disorders. The content is solely the responsibility of the authors and does not represent the official views of these institutes.

REFERENCES

1. Hardy M. The length of the organ of corti in man. *Am J Anat.* 1938; 63:291–311.
2. Walby AP. Scala tympani measurement. *Ann Otol Rhinol Laryngol.* 1985; 94:393–397. [PubMed: 3896104]
3. Ulehlová L, Voldrich L, Janisch R. Correlative study of sensory cell density and cochlear length in humans. *Hear Res.* 1987; 28:149–151. [PubMed: 3654386]
4. Wright A, Davis A, Friedberg G, Ulehlová L, Spencer H. Hair cell distributions in the normal human cochlea. *Acta Otolaryngol Suppl.* 1987; 444:1–48. [PubMed: 3482777]
5. Bredberg G, Teti A, Zambonin Zallone A, Lundevall E, Lurato S. Ultrastructural evaluation of the microslicing method for the study of temporal bone pathology. *Acta Otolaryngol Suppl.* 1987; 436:7–14. [PubMed: 3314328]
6. Ariyasu L, Galey FR, Hilsinger R Jr, Byl FM. Computer-generated three-dimensional reconstruction of the cochlea. *Otolaryngol Head Neck Surg.* 1989; 100:87–91. [PubMed: 2495514]
7. Kawano A, Seldon HL, Clark GM. Computer-aided three dimensional reconstruction in human cochlear maps: measurement of the lengths of organ of Corti, outer wall, inner wall, and Rosenthal's canal. *Ann Otol Rhinol Laryngol.* 1996; 105:701–709. [PubMed: 8800056]
8. Ketten DR, Skinner MW, Wang G, Vannier MW, Gates GA, Neely JG. In vivo measures of cochlear length and insertion depth of nucleus cochlear implant arrays. *Ann Otol Rhinol Laryngol Suppl.* 1998; 175:1–16. [PubMed: 9826942]
9. Adunka O, Unkelbach MH, Mack MG, Radloff A, Gstoettner W. Predicting basal cochlear length for electric-acoustic stimulation. *Arch Otolaryngol Head Neck Surg.* 2005; 131:488–492. [PubMed: 15967880]
10. Miller JD. Sex differences in the length of the Organ of Corti in humans. *J Acoust Am.* 2007; 121:151–155.
11. Erixon E, Hogstorp H, Wadin K, Rask-Andersen H. Variational anatomy of the human cochlea: implications for cochlear implantation. *Otol Neurotol.* 2009; 30:14–22. [PubMed: 18833017]
12. Lee J, Nadol JB Jr, Eddington DK. Depth of electrode insertion and postoperative performance in humans with cochlear implants: a histopathologic study. *Audiol Neurootol.* 2010; 15:323–331. [PubMed: 20203481]
13. Yukawa K, Cohen L, Blamey P, Pyman B, Tungvachirakul V, O'Leary S. Effects of insertion depth of cochlear implant electrodes upon speech perception. *Audiol Neurootol.* 2004; 9(3):163–172. [PubMed: 15084821]
14. Skinner MW, Ketten DR, Holden LK, et al. CT-derived estimation of cochlear morphology and electrode array position in relation to word recognition in nucleus-22 recipients. *J Assoc Res Otolaryngol.* 2002; 3(3):332–350. [PubMed: 12382107]
15. Hochmair I, Arnold W, Nopp P, Jolly C, Muller J, Roland P. Deep electrode insertion in cochlear implants: Apical morphology, electrodes and speech perception results. *Acta Otolaryngol.* 2003; 123(5):612–617. [PubMed: 12875584]
16. O'Connell BP, Cakir A, Hunter JB, Francis DO, Noble JH, Labadie RF, Zuniga G, Dawant BM, Rivas A, Wanna GB. Electrode Location and Angular Insertion Depth Are Predictors of Audiologic Outcomes in Cochlear Implantation. *Otol Neurotol.* 2016 Sep; 37(8):1016–1023. [PubMed: 27348391]
17. Alexiades G, Dhanasingh A, Jolly C. Method to estimate the complete and two-turn cochlear duct length. *Otol Neurotol.* 2015; 36(5):904–907. [PubMed: 25299827]
18. Noble JH, Labadie RF, Majdani O, Dawant BM. Automatic segmentation of intracochlear anatomy in conventional CT. *IEEE Trans Biomed Eng.* 2011; 58(9):2625–2632. [PubMed: 21708495]
19. Escude B, James C, Deguine O, Cochard N, Eter E, Fraysse B. The size of the cochlea and predictions of insertion depth angles for cochlear implant electrodes. *Audiol Neurootol.* 2006; 11(Suppl 1):27–33. [PubMed: 17063008]

20. Verbist BM, Skinner MW, Cohen LT, Leake PA, James C, Boëx C, Holden TA, Finley CC, Roland PS, Roland JT Jr, Haller M. Consensus panel on a cochlear coordinate system applicable in histological, physiological and radiological studies of the human cochlea. *Otology & neurotology: official publication of the American Otological Society, American Neurotology Society [and] European Academy of Otology and Neurotology*. 2010 Jul.31(5):722.
21. Schuman TA, Noble JH, Wright CG, Wanna GB, Dawant B, Labadie RF. Anatomic verification of a novel method for precise intrasclerous localization of cochlear implant electrodes in adult temporal bones using clinically available computed tomography. *Laryngoscope*. 2010; 120(11):2277–2283. [PubMed: 20939074]
22. Goshtasby A. Registration of Images with Geodesic Distortion. *IEEE Transactions on Geoscience and Remote Sensing*. 1988 Jan.26(1):60–64.
23. O'Connell BP, Cakir A, Hunter JB, Francis DO, Noble JH, Labadie RF, Zuniga G, Dawant BM, Rivas A, Wanna GB. Electrode Location and Angular Insertion Depth Are Predictors of Audiologic Outcomes in Cochlear Implantation. *Otol Neurotol*. 2016; 37(8):1016–1023. [PubMed: 27348391]
24. Peterson GE, Lehist I. Revised CNC Lists for Auditory Tests. *Jour. of Speech and Hear. Disord*. 1962; 27:62–70. [PubMed: 14485785]

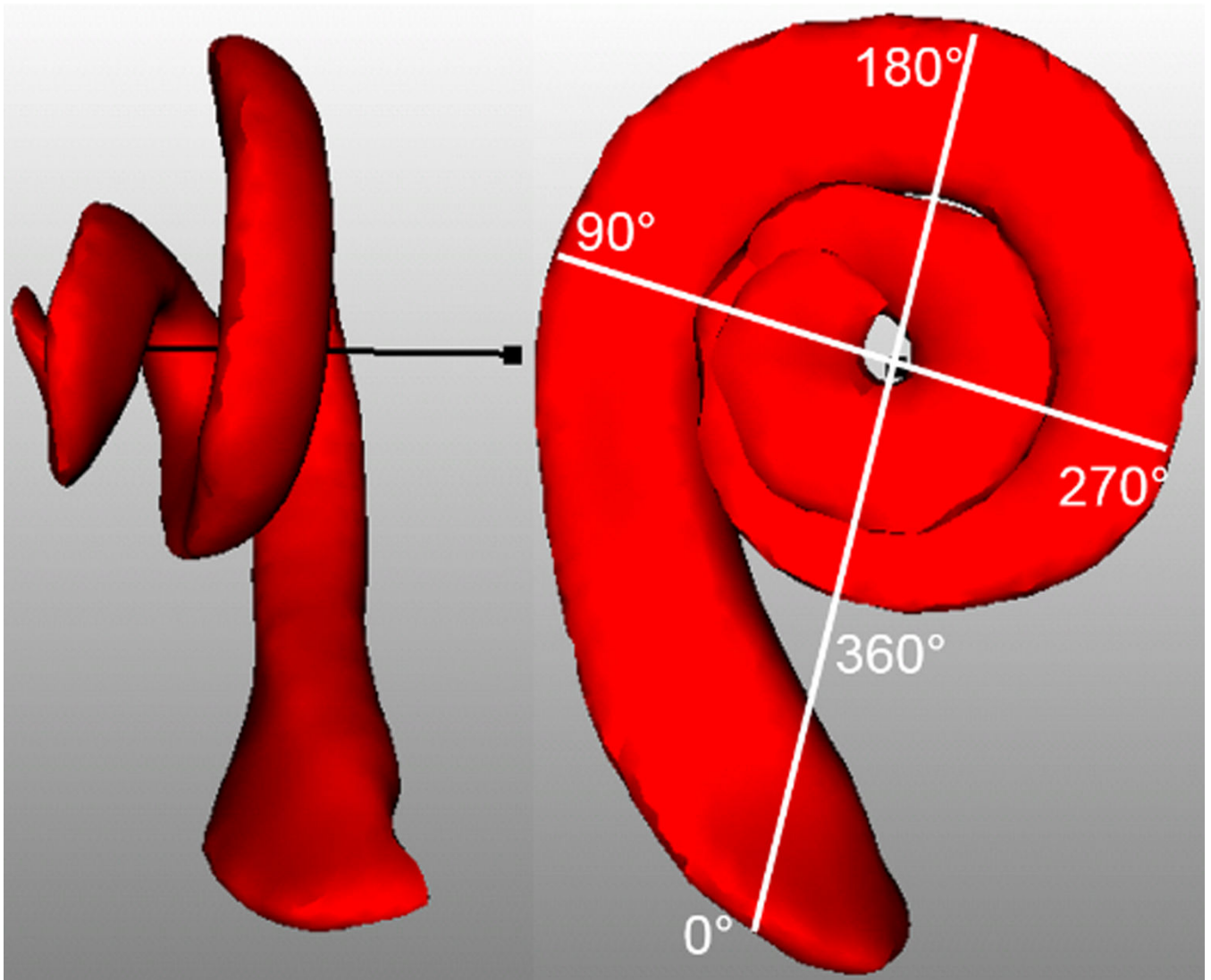


Figure 1. Explanation of angular depth. Scala Tympani is shown in red and mid-modiolar axis is shown in black. Round Window (RW) is marked with 0°

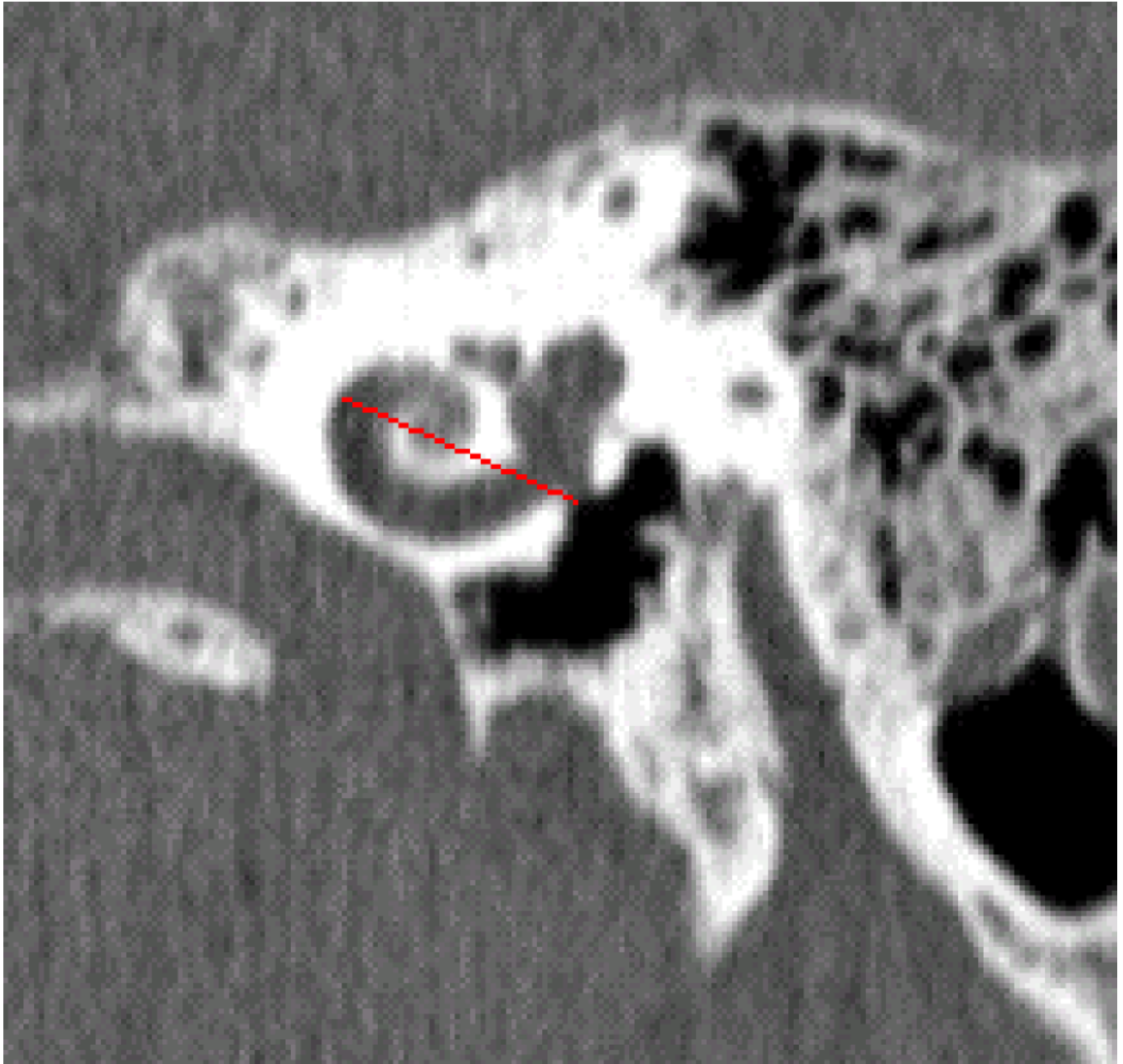


Figure 2.
Example of manual selection of *A*

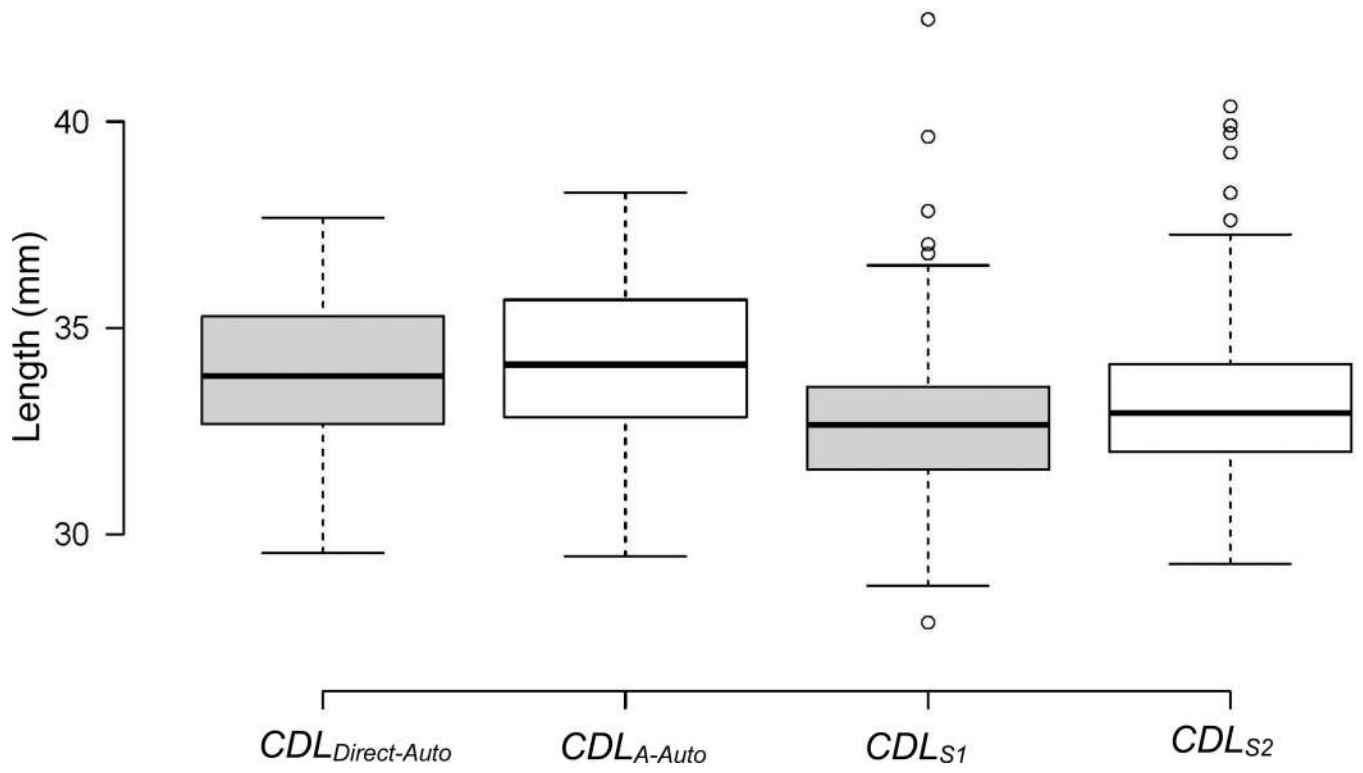


Figure 3.
Box plots of the automatically measured and the estimated CDL

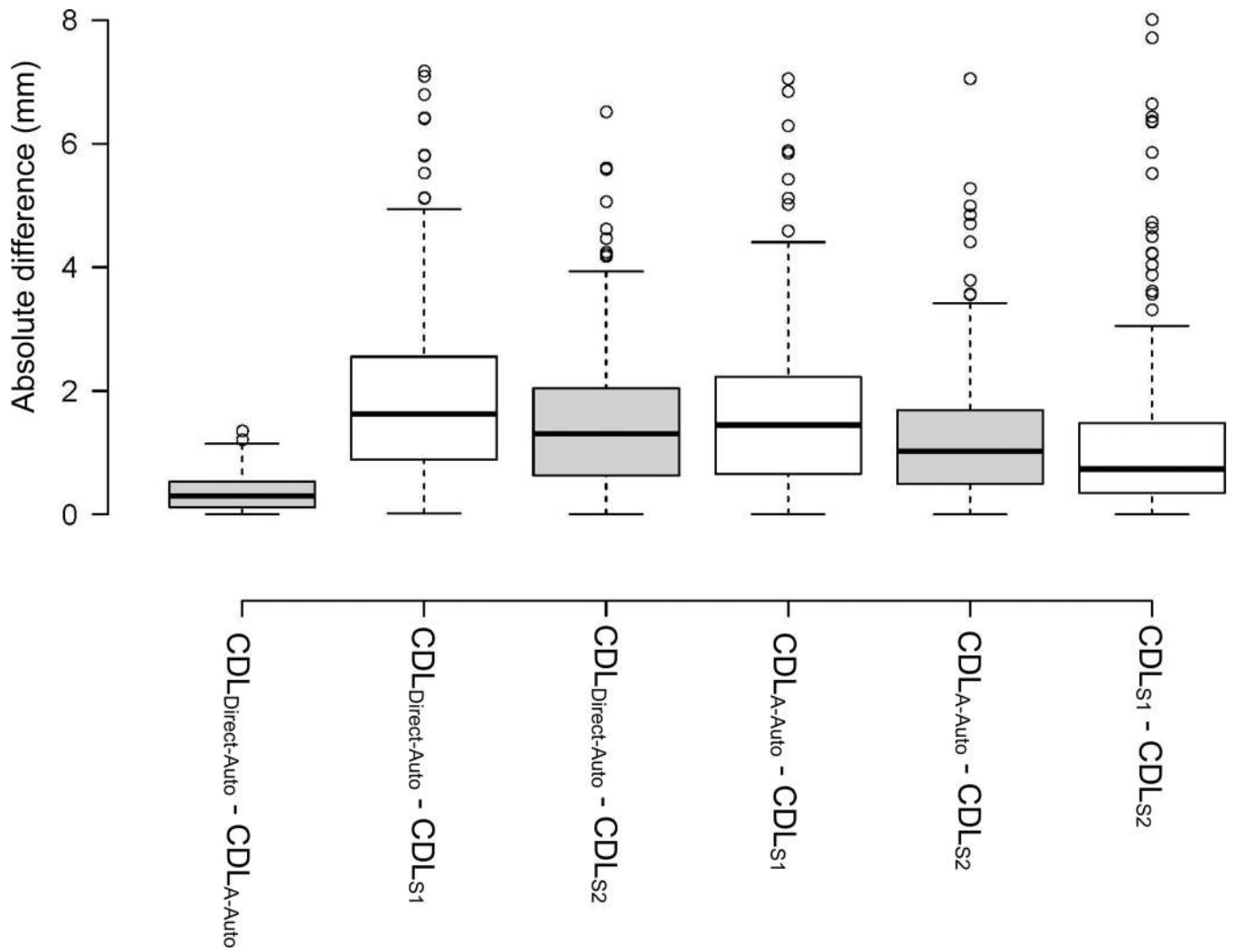


Figure 4. Box plots of the difference between all of the four different cochlear duct length (CDL) values

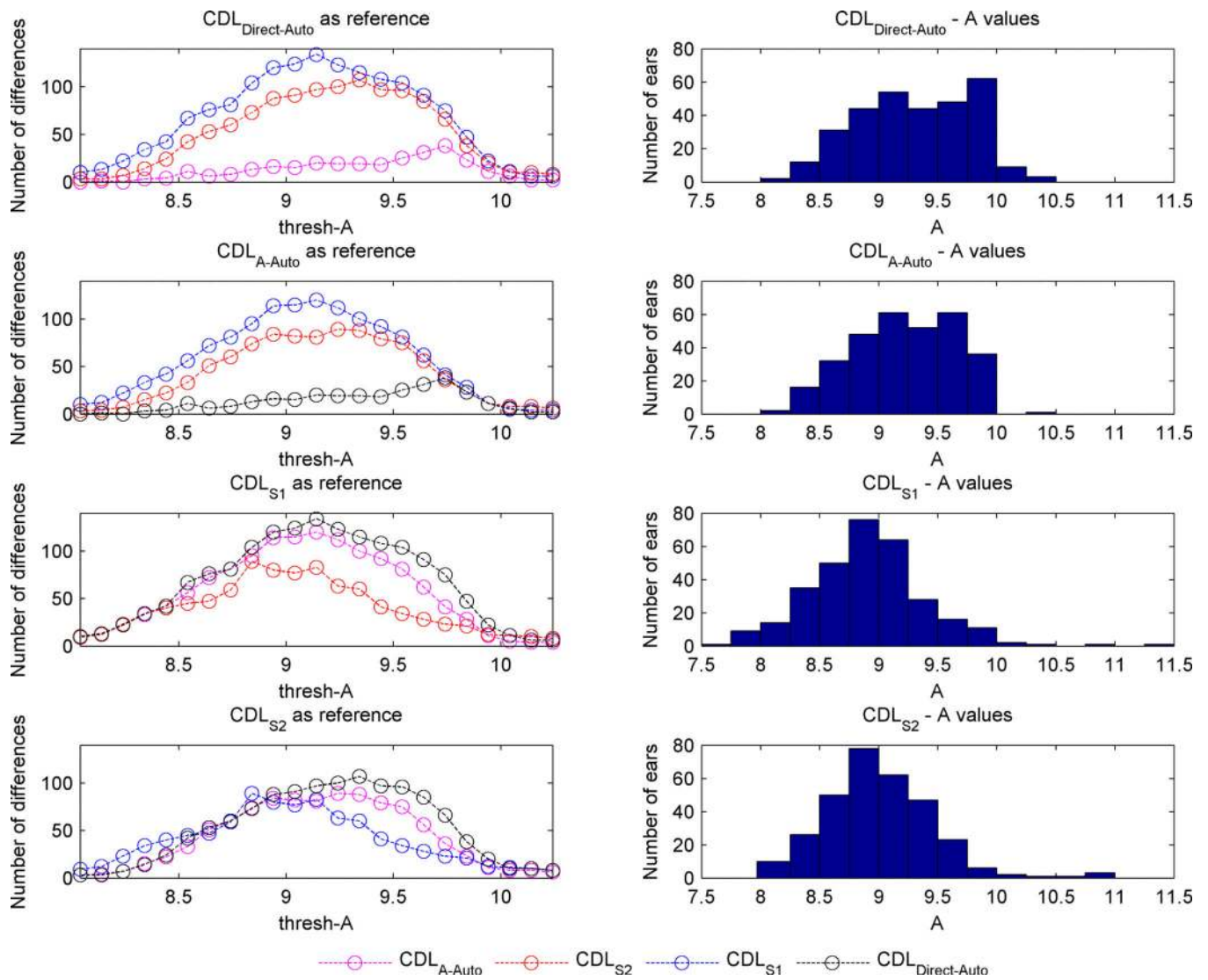


Figure 5. Panels in the left column show the number of times the selected electrode arrays differed among measurement methods for different values of *thresh-A*. Right columns show histograms of cochlea size across subjects using each measurement technique.

Table 1Maximum, minimum, mean and standard deviation across automatically and manually measured *A* values

	Maximum (mm)	Minimum (mm)	Mean ± standard deviation (mm)
A_{Auto}	10.25	8.04	9.22 ± 0.44
A_{S1}	11.56	7.58	8.91 ± 0.49
A_{S2}	10.99	7.97	9.00 ± 0.46

Author Manuscript

Author Manuscript

Author Manuscript

Author Manuscript